The predictions of the charm structure function exponents behaviour at low x in deep inelastic scattering

G.R.Boroun[1] and B.Rezaei[1]

[1] *Physics Department, Razi University, Kermanshah 67149, Iran*

arXiv:1402.0165v1 [hep-ph] 2 Feb 2014

PACS 13.60.Hb – First pacs description
PACS 12.38.Bx – Second pacs description

Abstract – We use the hard (Lipatov) pomeron for the low x gluon distribution and provide a compact formula for the ratio $R^c = \frac{F_L^{c\overline{c}}}{F_2^{c\overline{c}}}$ that is useful to extract the charm structure function from the reduced charm cross section, in particular at DESY HERA. Our results show that this ratio is independent of x and independent of the DGLAP evolution of the gluon PDF. As a result, we show that the charm structure function and the reduced charm cross section exponents do not have the same behaviour at very low x. This difference is independent of the input gluon distribution functions and predicts the non- linear effects and some evidence for shadowing and antishadowing at HERA and RHIC.

1. INTRODUCTION. – Precise measurements of the charm inclusive scattering cross section at the *ep* collider are important for the understanding of charmed meson production. In the one-photon exchange approximation the neutral current, charmed meson production in deeply inelastic *ep* scattering is via this reaction

$$e^- + P \to e^- + c\overline{c} + X. \tag{1}$$

In the case of pure photon exchange, the totally inclusive cross section of the deep-inelastic lepton-proton scattering (DIS) has the form:

$$\frac{d^2\sigma}{dxdQ^2} = \frac{2\pi\alpha^2 Y_+}{Q^4 x}.\sigma_r, \tag{2}$$

where the reduced cross section is defined as

$$\sigma_r \equiv F_2(x,Q^2) - \frac{y^2}{Y_+}.F_L(x,Q^2), \tag{3}$$

and $Y_+ = 1 + (1-y)^2$. Here Q^2 is the squared four-momentum transfer, x denotes the Bjorken scaling variable, $y = Q^2/sx$ is the inelasticity, with s the ep center of mass energy squared, and α is the fine structure constant. The structure functions F_2 and F_L are related to the cross sections σ_T and σ_L for interaction of transversely and longitudinally polarized virtual photons with protons [1]. At small values of x, F_L becomes non-negligible and its contribution should be properly taken into account when the F_2 is extracted from the measured cross section. However, the contribution of the longitudinal structure function F_L to the cross section is sizeable only at large values of the inelasticity y, in most of the kinematic range the relation $\sigma_r \approx F_2$ holds to a very good approximation. The same is true also for the contributions $F_2^{c\overline{c}}$ and $F_L^{c\overline{c}}$ to F_2 and F_L due to the charm quarks.

In perturbative QCD (pQCD) calculations, the production of heavy quarks at HERA proceeds dominantly via the direct boson-gluon fusion (BGF) where the photon interacts with a gluon from the proton by the exchange of a heavy quark pair [2]. Charm production contribution to the DIS cross section data was found to be around 30% F_2 at HERA [3,4]. The deeply inelastic heavy-flavour structure function contribution to the cross section is given by

$$\begin{aligned}\sigma_r^{c\overline{c}} &= \frac{Q^4 x}{2\pi\alpha^2 Y_+}\frac{d^2\sigma^{c\overline{c}}}{dxdy} \\ &= F_2^{c\overline{c}}(x,Q^2,m^2) - \frac{y^2}{Y_+}F_L^{c\overline{c}}(x,Q^2,m^2) \\ &= F_2^{c\overline{c}}(x,Q^2,m^2)(1-\frac{y^2}{Y_+}R^c).\end{aligned} \tag{4}$$

A measurement of the longitudinal charm structure function at low x at HERA is important because the $F_L^{c\overline{c}}$ contribution to the charm cross section can be sizeable.

At small values of x, $F_L^{c\overline{c}}$ becomes non-negligible and its contribution should be properly taken into account when the $F_2^{c\overline{c}}$ is extracted from the measured charm cross section. This has been done, for example for H1 charm data, by making an NLO QCD fit in the DGLAP formalism such that the correction necessary for $F_L^{c\overline{c}}$ is calculated in this formalism. Instead of this procedure, we propose to use the expression 4 with the quantity R^c determined in NLO approximation, which has the advantage of being independent of the gluon PDF. This simplifies the extraction of $F_2^{c\overline{c}}$ from measurements of $\sigma_r^{c\overline{c}}$.

In this paper, the charm structure function is evaluated from the charm reduced cross section (4) where the ratio of the charm structure functions, R^c, is calculated in a more robust NLO approximation. We propose to use the hard (Lipatov)Pomeron behaviour of the charm structure functions and determine the ratio of the charm structure functions $R^c = \frac{F_L^{c\overline{c}}}{F_2^{c\overline{c}}}$ from this behaviour in the limit of low $x\to 0$. Assuming the low x asymptotic behaviour of the gluon PDF to be of the type $G(x,Q^2)\propto 1/x^\delta$ ($G(x,Q^2) = xg(x,Q^2)$), we provide numerical results for the ratio $R(x\to 0,Q^2)\equiv R_\delta(Q^2)$ for values of the parameter $\delta = 0$ or $\delta = 0.5$, the first value corresponds to the soft Pomeron and the second value is corresponding to the hard (Lipatov) Pomeron intercept. However, our analysis shows that the predictions for R^c with hard Pomeron intercept describe with good accuracy the low x predictions to NLO, and this analysis is independent of the DGLAP evolution of the gluon PDF. In this method, the charm structure function is determined without the prior knowledge of the longitudinal charm structure function.
Finally, our predictions show that the charm structure function exponents have the same behaviour as the reduced charm cross section exponents only for a particular range of x values. The structure of this article is as follows. In Sect.2 we present the basic formalism of our approximation method with a brief review of the calculational steps. The connection of the ratio of the charm structure functions with hard (Lipatov) Pomeron intercept is also given. Later, we present the results for the charm structure function with NLO corrections and show that our method reproduces the HERA results for the charm structure function obtained by H1 Collaboration with the help of more cumbersome NLO estimations. In Sect.3 we give the predictions for the charm structure function exponents with respect to the reduced charm cross section exponents at low x. These results are discussed in Sect.4.

2. The Hard (Lipatov) Pomeron Approach to the charm structure functions . – In the low- x range, where the gluon contribution is dominant, the charm quark contribution $F_k^c(x,Q^2,m_c^2)(k=2,L)$ to the proton structure function is given by this form

$$F_k^c(x,Q^2,m_c^2) = 2e_c^2\frac{\alpha_s(\mu^2)}{2\pi}\int_{1-\frac{1}{a}}^{1-x} dz C_{g,k}^c(1-z,\zeta) \times G(\frac{x}{1-z},\mu^2), \quad (5)$$

where $a = 1+4\zeta(\zeta\equiv\frac{m_c^2}{Q^2})$ and we neglect the $\gamma^* q(\overline{q})$ fusion subprocesses. Here $G(x,\mu^2)$ is the gluon distribution function and the mass factorization scale μ, which has been put equal to the renormalization scale, is assumed to be either $\mu^2 = 4m_c^2$ or $\mu^2 = 4m_c^2+Q^2$. In the above expression $C_{g,k}^c$ is the charm coefficient function expressed in terms of LO and NLO contributions as follows

$$C_{k,g}(z,\zeta) \to C_{k,g}^0(z,\zeta) + a_s(\mu^2)[C_{k,g}^1(z,\zeta) + \overline{C}_{k,g}^1(z,\zeta)\ln\frac{\mu^2}{m_c^2}], \quad (6)$$

where $a_s(\mu^2) = \frac{\alpha_s(\mu^2)}{4\pi}$ and in the NLO analysis

$$\alpha_s(\mu^2) = \frac{4\pi}{\beta_0\ln(\mu^2/\Lambda^2)} - \frac{4\pi\beta_1}{\beta_0^3}\frac{\ln\ln(\mu^2/\Lambda^2)}{\ln(\mu^2/\Lambda^2)} \quad (7)$$

with $\beta_0 = 11-\frac{2}{3}n_f, \beta_1 = 102-\frac{38}{3}n_f$ (n_f is the number of active flavours).

In the LO analysis, the coefficient functions BGF can be found [5-8], as

$$C_{g,2}^0(z,\zeta) = \frac{1}{2}([z^2+(1-z)^2+4z\zeta(1-3z)-8\zeta^2z^2] \times\ln\frac{1+\beta}{1-\beta}+\beta[-1+8z(1-z) -4z\zeta(1-z)]), \quad (8)$$

and

$$C_{g,L}^0(z,\zeta) = -4z^2\zeta\ln\frac{1+\beta}{1-\beta}+2\beta z(1-z), \quad (9)$$

where $\beta^2 = 1-\frac{4z\zeta}{1-z}$.
At NLO, $O(\alpha_{em}\alpha_s^2)$, the contribution of the photon- gluon component is usually presented in terms of the coefficient functions $C_{k,g}^1, \overline{C}_{k,g}^1$. The NLO coefficient functions are only available as computer codes[9,10]. But in the high-energy regime ($\zeta << 1$) we can used the compact form of these coefficients according to the Refs.[11,12].

Applying the low- x behaviour of the gluon distribution function according to the hard (Lipatov) Pomeron [13-15]

$$G(x,\mu^2)\to x^{-\delta} \quad (10)$$

in Eq.5, integrating the gluon kernel over $z = \frac{x}{y}$ and finally summing over the gluon distribution function yields

$$F_k^c(x,Q^2,m_c^2) = 2e_c^2\frac{\alpha_s(\mu^2)}{2\pi}N_k(x,\mu^2) \times G(x,\mu^2), \quad (11)$$

where

$$N_k(x,\mu^2)=\int_{1-\frac{1}{a}}^{1-x} C^c_{g,k}(1-z,\zeta)(1-z)^{\delta}dz. \qquad (12)$$

Therefore the ratio of the charm structure functions is given by

$$\begin{aligned} R^c &= \frac{F_L^c}{F_2^c} \\ &= \frac{N_L(x,\mu^2)}{N_2(x,\mu^2)}, \end{aligned} \qquad (13)$$

In fact, this equation which is independent of the gluon distribution function, is very useful for practical applications.
We insert this expression in Eq.4 to find

$$\sigma_r^{c\overline{c}}=F_2^{c\overline{c}}(x,Q^2,m^2)(1-\frac{y^2}{Y_+}\frac{N_L(x,\mu^2)}{N_2(x,\mu^2)}), \qquad (14)$$

or

$$F_2^{c\overline{c}}(x,Q^2,m^2)=\sigma_r^{c\overline{c}}(1-\frac{y^2}{Y_+}\frac{N_L(x,\mu^2)}{N_2(x,\mu^2)})^{-1}. \qquad (15)$$

This equation relates the charm structure function to the reduced charm structure function via BGF kernels. We observe that the right- hand side of Eq.15 is independent of the longitudinal charm structure function and gluon distribution function, and this formula can reproduce the HERA results for the charm structure function from the reduced charm cross section.

3. The charm structure function exponent behaviour . – A striking discovery at HERA [2] for the charm productions has been the rapid rise of $\sigma_r^{c\overline{c}}$ with the energy W^2 at each fixed Q^2 and small x values. This rapid rise is associated with the exchange of an object known as the hard (Lipatov) Pomeron. In this powerful approach the charm structure function has been found to have the same hard (Lipatov) Pomeron behaviour [16-18]. This rise has been quantified by a study of the observable

$$\lambda_{F_2^{c\overline{c}}}=\langle\frac{\partial \ln F_2^{c\overline{c}}}{\partial \ln 1/x}\rangle \qquad (16)$$

where the brackets mean that this effective intercept ($\lambda_{F_2^{c\overline{c}}}$) is obtained from a fit of the form $F_2^{c\overline{c}}\sim x^{-\lambda_{F_2^{c\overline{c}}}}$ at fixed Q^2 and small values of x. We analyse the H1 $\sigma_r^{c\overline{c}}$ data with a view to extracting such an x dependence. For this purpose, from Eq.4, we have the following form

$$\langle\frac{\partial \ln \sigma_r^{c\overline{c}}}{\partial \ln 1/x}\rangle=\langle\frac{\partial \ln F_2^{c\overline{c}}}{\partial \ln 1/x}\rangle+\langle\frac{\partial \ln[1-\frac{y^2}{Y_+}R^c]}{\partial \ln 1/x}\rangle. \qquad (17)$$

We would like remark that

$$\lambda_{\sigma_r^{c\overline{c}}}=\lambda_{F_2^{c\overline{c}}}+\Delta\lambda \qquad (18)$$

where

$$\Delta\lambda=\frac{R^c}{1-\frac{y^2}{Y_+}R^c}\frac{\partial}{\partial \ln 1/x}\frac{y^2}{Y_+}, \qquad (19)$$

or

$$\begin{aligned} \Delta\lambda &= -2(2sx-Q^2)R^c sQ^4x[(2s^2x^2-2sxQ^2+Q^4-Q^4R^c) \\ &\times(2s^2x^2-2sxQ^2+Q^4)]^{-1}. \end{aligned} \qquad (20)$$

Here s is the square of the total c.m. energy (which is constant at HERA). As shown in Fig.1, the R^c behaviour is almost independent of x at all Q^2 values. $\Delta\lambda$ is independent of the gluon distribution, depending only on the BGF kernels. We shall analyse it for both small and large y data.

4. Results and Conclusions . – We have analysed H1 data on charm production [3] and compared with DL model [16-18] based on hard Pomeron exchange and also with the color dipole- model [19] and the GJR parametrisation [23]. Our numerical predictions are presented as functions of x for the Q^2 =12,20,35,60, 120 and 200 GeV^2. The ep center of mass energy is $\sqrt{s}=319GeV$, with a proton beam energy of $E_p=920GeV$ and electron beam energy of $E_e=27.6GeV$ and also the average value Λ in our calculations is corresponding to 224 MeV.

In Figs.1 and 2 we show the predicted ratio of the charm structure functions, R^c, as a function of x and Q^2. As can be seen from these figures R^c is almost independent of x for $x<0.01$ in all Q^2 region. Also it is independent on the choice of the gluon distribution function, where approaches based on perturbative QCD and on k_T factorization give similar predictions [20-22]. The effect of R^c on the corresponding differential charm cross- section should be considered in extraction of F_2^c, so in Table 1 we give the average of this ratio for various Q^2 values. We see $\langle R^c\rangle\approx 0.1$ for a wide region of Q^2. In principle, the parameter δ has two value $\delta=0.08$ and $\delta=0.44$. The first one is corresponds to soft- pomeron exchange and the second one is corresponds to hard-pomeron exchange. Our analysis shows that the predictions for R^c depend weakly on δ, as it is less than 15% in the entire region of Q^2. Therefore, our approximation method for R^c with hard-pomeron behaviour describes with good accuracy the low x predictions for R^c when compared with results Ref.11 at NLO analysis (Fig.1 in Ref.11).

Now we use the analytic expression (15) for the extraction of the charm structure function $F_2^c(x,Q^2)$ from the $H1$ measurements of the reduced cross section using the NLO results for R^c derived in Section 2. Our results for the charm structure function are presented in Table 2 and shown in Fig.3, where they are compared with the values determined by the $H1$ analysis and with results obtained with the help of other standard models (DL fit [16-18],

color dipole model [19] and GJR parametrization [23]). The agreement between our predictions with the results obtained by H1 Collaboration is remarkably good. Also we observed that the theoretical uncertainty related to the renormalization scales $\mu^2 = 4m_c^2$ and $\mu^2 = 4m_c^2 + Q^2$ is negligibly small. Our results for extraction of the charm structure function from HERA measurements of the reduced charm cross section are given for both the hard and soft pomeron behaviour for δ. One can see that the predictions of our NLO analysis for the hard and soft pomeron behaviour agree with the H1 data with an accuracy better than 1%. This is because the contributions of the longitudinal charm structure function to the reduced charm cross section is very small. The numerical results show that a rough estimate of the uncertainty in the charm structure function due to the difference between the assumptions of a soft or a hard pomeron is less than 0.2%.

Finally, we analyse the behaviour of the exponents for the charm structure function and the reduced charm cross section. To begin with, we recognise that the behaviour of $\Delta\lambda$ (Eq.20) is independent of the input gluon distribution function. The behaviour of this expression as a function of x (or y) is shown in Fig.4 for several values of Q^2 (Q^2 and s are constant). We observe that the behaviour of $\Delta\lambda$ at low y (or high x) values is linear, $\Delta\lambda$ is very small so that $\lambda_{F_2^{c\bar{c}}} \simeq \lambda_{\sigma_r^{c\bar{c}}}$, and this quantity can be determined from derivatives of the $\sigma_r^{c\bar{c}}$ experimental data with respect of $\ln 1/x$ at Q^2 fixed. But in the large y region (low x), $\Delta\lambda$ can no longer be neglected. The deviation of this expression from zero shows the importance of non-linear effects. Thus we observe that for large x (low y) there are not saturation effects. In this region the behaviour of the charm structure function exponent and reduced charm cross section exponent is the same and the hard (Lipatov) pomeron picture gives a good fit to all data. A depletion in the low x (high y) is called shadowing whereas an enhancement is called anti-shadowing [24].

The oscillating behaviour for $\Delta\lambda$ in Fig.4 can be explained by new effects at low-x, such as the behaviour of the gluon distribution evaluated with the nonlinear recombination. The negative shadowing corrections to this behaviour can be explain by the gluon recombination. This negative screening effect in the recombination process originally occurs in the interferant cut- diagrames of the recombination amplitudes. But the positive anti-shadowing corrections comes from a general application of momentum conservation. This anti- shadowing effect always coexists with the shadowing effect in the QCD recombination processes. Therefore we observe that significant non- linear effects to the modified DGLAP equation for the charm structure function can be apparent in the behaviour of the charm structure function exponent. This shadowing and anti- shadowing effects in the $\Delta\lambda$ behaviour have different kinematic regions. The net effects for $\Delta\lambda$ behaviour depends not only on the size of gluon distribution at this value of x in the modified DGLAP equation for the charm structure function, but also on the shape of the gluon distribution when the Bjorken variable goes from x to $x/2$. In consequence, the shadowing effects in the exponents behaviour will be obviously weakened by the antishadowing effects as the gluon distribution has a steeper behavior at low-x values. This transition for $\Delta\lambda$ is shown in Fig.4. The main prediction is a transition from the linear regime described for the exponents to a non-linear regime where parton recombination becomes important in the parton cascade. In view of these results for the exponents, we may infer some evidence for non- linear effects at HERA and RHIC.

In summary, we have used the hard (Lipatov) pomeron for the low x gluon distribution to predict the charm structure functions (F_2^c and F_L^c). We derived a compact formula for the ratio $R^c = \frac{F_L^{c\bar{c}}}{F_2^{c\bar{c}}}$ that is valid through NLO at small values of Bjorken's x variable, as it is independent of the input gluon distribution function. We have checked that this formula gives a good description of the charm structure function from the reduced charm cross section data without the prior knowledge of the longitudinal charm structure function. Careful investigation of our results show a good agreement with the previously published charm structure functions and other models. Then we have used it to predict the behaviour of the charm structure function and reduced charm cross section exponents in the Perturbative Q^2 region at small x. Our predictions indicate that the behaviour of $\Delta\lambda$ can be explained by non linear effects at very low x. These numerical results show that the correction of the modified DGLAP equation due to gluon recombination incorporates both shadowing and antishadowing effects, as the influence of the antishadowing effect to the pre-asymptotic form of the gluon distribution is non-negligible.

* * *

G.R.Boroun thanks Prof.A.Cooper-Sarkar for interesting and useful discussions.

REFERENCES

[1] .D.H.Perkins,Introduction to High Energy Physics,(University of Oxford,Oxford, England,1982),ADDISON-WESLEY PUBLISHING ; Francis Halzen and Alan D.Martin,Quarks and Leptons,(JOHN WILEY & SONS,1984).

[2] .K.Lipka, Pos(EPS-HEP),313(2009).

[3] . C. Adloff et al. [H1 Collaboration], Z. Phys. C**72**, 593 (1996); J. Breitweg et al. [ZEUS Collaboration], Phys. Lett. B**407**, 402 (1997); C. Adloff et al. [H1 Collaboration], Phys. Lett. B**528**, 199 (2002); S. Aid et. al., [H1 Collaboration], Z. Phys. C**72**, 539 (1996); J. Breitweg et. al., [ZEUS Collaboration], Eur. Phys. J. C**12**, 35 (2000); S. Chekanov et. al., [ZEUS Collaboration], Phys. Rev. D**69**, 012004 (2004); Aktas et al. [H1 Collaboration], Eur. Phys.J. C**45**, 23 (2006); F.D. Aaron et al. [H1 Collaboration],Eur.Phys.J.C**65**,89(2010).

[4] .N.Ya.Ivanov, Nucl.Phys.B814,142(2009).

[5] .V.N. Baier et al., Sov. Phys. JETP 23 104 (1966); V.G. Zima, Yad. Fiz. 16 1051 (1972); V.M. Budnev et al., Phys. Rept. 15 181 (1974).

[6] .E. Witten, Nucl. Phys. B104 445 (1976); J.P. Leveille and T.J. Weiler, Nucl. Phys. B147 147 (1979); V.A. Novikov et al., Nucl. Phys. B136 125 (1978) 125.

[7] .E. Witten, Nucl. Phys. B104 445 (1976); J.P. Leveille and T.J. Weiler, Nucl. Phys. B147 147 (1979); V.A. Novikov et al., Nucl. Phys. B136 125 (1978) 125.

[8] .A.Vogt, arXiv:hep-ph:9601352v2(1996).

[9] . E.Laenen, S.Riemersma, J.Smith and W.L. van Neerven, Nucl.Phys.B **392**, 162(1993).

[10] .M.Gluk, E.Reya and A.Vogt, Z.Phys.C**67**, 433(1995); Eur.Phys.J.C**5**, 461(1998).

[11] . A. Y. Illarionov,B. A. Kniehl and A. V. Kotikov, Phys.Lett. B **663**, 66 (2008).

[12] . S. Catani, M. Ciafaloni and F. Hautmann, Preprint CERN-Th.6398/92, in Proceeding of the Workshop on Physics at HERA (Hamburg, 1991), Vol. 2., p. 690; S. Catani and F. Hautmann, Nucl. Phys. B **427**, 475(1994); S. Riemersma, J. Smith and W. L. van Neerven, Phys. Lett. B **347**, 143(1995).

[13] . N.Nikolaev, J.Speth and V.R.Zoller,Phys.Lett.B**473**, 157(2000).

[14] . R.Fiore, N.Nikolaev and V.R.Zoller,JETP Lett**90**, 319(2009).

[15] . I.P.Ivanov and N.Nikolaev,Phys.Rev.D**65**,054004(2002).

[16] . A.Donnachie and P.V.Landshoff, Z.Phys.C **61**, 139(1994); Phys.Lett.B **518**, 63(2001); Phys.Lett.B **533**, 277(2002); Phys.Lett.B **470**, 243(1999); Phys.Lett.B **550**, 160(2002).

Table 1: The predictions for the ratio $R^c = \frac{F_L^c}{F_2^c}$ as a function of Q^2 corresponding to the cases of hard and soft pomeron.

$Q^2(GeV^2)$	$< R^c > (\delta \simeq 0.5)$	$< R^c > (\delta \simeq 0)$
12	0.078	0.066
20	0.092	0.078
35	0.103	0.089
60	0.109	0.094
120	0.111	0.097
200	0.109	0.096
300	0.106	0.094
600	0.101	0.090
1000	0.096	0.086
10000	0.078	0.071
100000	0.065	0.061

[17] . R.D.Ball and P.V.landshoff, J.Phys.G**26**, 672(2000).

[18] . P.V.landshoff, arXiv:hep-ph/0203084 (2002).

[19] . N.N.Nikolaev and V.R.Zoller, Phys.Lett. B**509**, 283(2001).

[20] . A. V. Kotikov, A. V. Lipatov, G. Parente and N. P. Zotov Eur. Phys. J. C **26**, 51 (2002).

[21] . V. P. Goncalves and M. V. T. Machado, Phys. Rev. Lett. **91**, 202002 (2003).

[22] . N.Ya.Ivanov, Nucl.Phys.B**814** , 142 (2009); Eur.Phys.J.C **59**, 647(2009).

[23] . M. Gluck, P. Jimenez-Delgado, E. Reya, Eur.Phys.J.C **53**,355 (2008).

[24] . W.Zhu, et.al., Nucl.Phys.B **551**, 245(1999); Nucl.Phys.B **559**, 375(1999); J.Ruan, et.al., Nucl.Phys.B **760**, 128(2007).

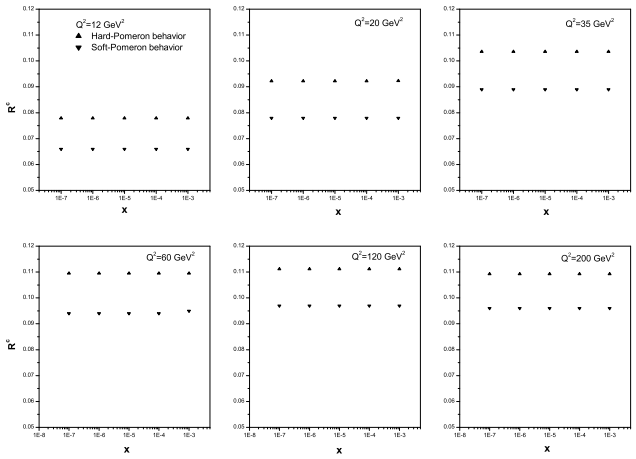

Fig. 1: The ratio $R^c = \frac{F_L^{c\bar{c}}}{F_2^{c\bar{c}}}$ as a function of x for different values of Q^2 at $\delta \simeq 0$ and $\delta \simeq 0.5$.

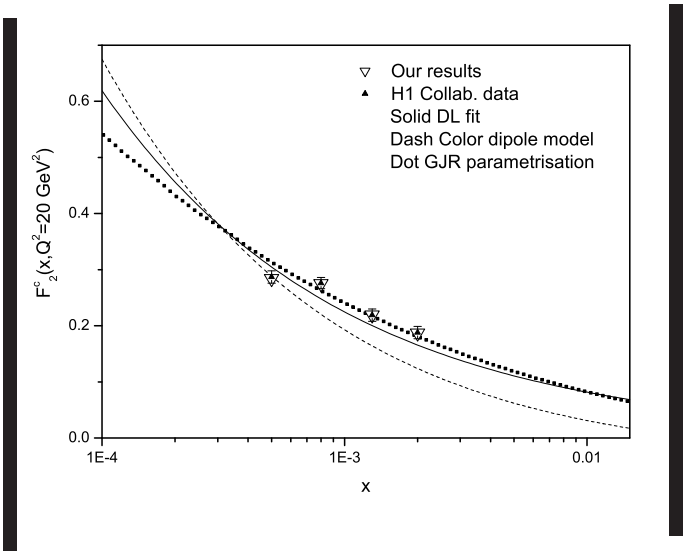

Fig. 3: The structure function $F_2^c(x, Q^2)$ as a function of x at $Q^2 = 20GeV^2$ compared with HERA data that accompanied with total errors (F.D. Aaron et al.,Eur.Phys.J.C**65**,89(2010)) [3], DL fit [16-18], color dipole model[19] and GJR parametrisation [23].

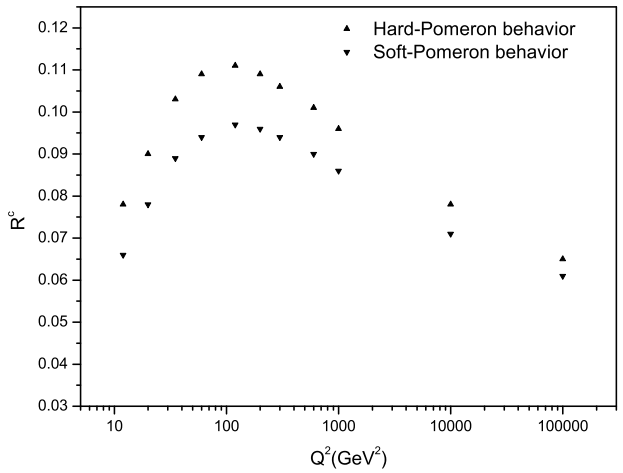

Fig. 2: The ratio $R^c = \frac{F_L^{c\bar{c}}}{F_2^{c\bar{c}}}$ as a function of Q^2 values at $\delta \simeq 0$ and $\delta \simeq 0.5$.

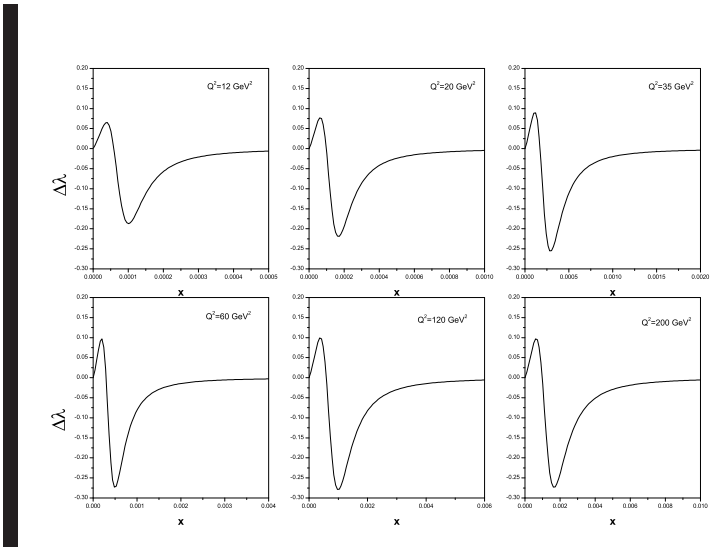

Fig. 4: The nonlinear behaviour of the exponents ($\Delta\lambda = \lambda_{F_2^{c\bar{c}}} - \lambda_{\sigma_r^{c\bar{c}}}$) as a function of x at Q^2 values.

Table 2: The values of $F_2^c(x,Q^2)$ corresponding to the hard-pomeron behaviour extracted from the $\widetilde{\sigma}^c(x,Q^2)$ at low and high Q^2 for various values of x are compared with H1 results [3] that accompanied with total errors ($\Delta\%$).

$Q^2(GeV^2)$	x	y	$\widetilde{\sigma}^{c\overline{c}}$	$\Delta_{\widetilde{\sigma}^{c\overline{c}}}(\%)$	$F_2^{c\overline{c}}$(Ref.3)	$\Delta_{F_2^{c\overline{c}}}(\%)$	$F_2^{c\overline{c}}(\delta \simeq 0.5)$	$F_2^{c\overline{c}}(\delta \simeq 0)$
12	0.00130	0.091	0.150	18.7	0.150	1.0	0.1500	0.1500
12	0.00080	0.148	0.177	15.9	0.177	1.1	0.1772	0.1771
12	0.00050	0.236	0.240	11.2	0.242	1.0	0.2407	0.2405
12	0.00032	0.369	0.273	13.8	0.277	1.1	0.2751	0.2747
20	0.00200	0.098	0.187	12.7	0.188	1.1	0.1871	0.1871
20	0.00130	0.151	0.219	11.9	0.219	1.1	0.2193	0.2192
20	0.00080	0.246	0.274	10.2	0.276	1.0	0.2750	0.2748
20	0.00050	0.394	0.281	13.8	0.287	1.1	0.2840	0.2834
35	0.00320	0.108	0.200	12.7	0.200	1.1	0.2001	0.2001
35	0.00200	0.172	0.220	11.8	0.220	1.0	0.2204	0.2203
35	0.00130	0.265	0.295	9.70	0.297	1.0	0.2964	0.2962
35	0.00080	0.431	0.349	12.7	0.360	1.1	0.3541	0.3533
60	0.00500	0.118	0.198	10.8	0.199	1.1	0.1982	0.1981
60	0.00320	0.185	0.263	8.40	0.264	1.0	0.2636	0.2635
60	0.00200	0.295	0.335	8.80	0.339	1.0	0.3372	0.3368
60	0.00130	0.454	0.296	15.1	0.307	1.0	0.3012	0.3004
120	0.01300	0.091	0.133	14.1	0.133	1.2	0.1331	0.1330
120	0.00500	0.236	0.218	11.1	0.220	1.1	0.2190	0.2187
120	0.00200	0.591	0.351	12.8	0.375	2.9	0.3630	0.3612
200	0.01300	0.151	0.161	11.9	0.160	2.7	0.1602	0.1612
200	0.00500	0.394	0.237	13.5	0.243	2.9	0.2400	0.2396
300	0.02000	0.148	0.117	18.5	0.117	2.9	0.1171	0.1171
300	0.00800	0.369	0.273	12.7	0.278	2.9	0.2760	0.2755